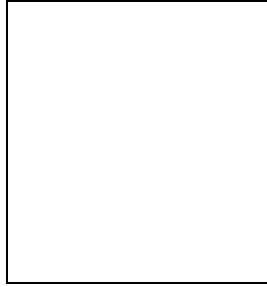


DALITZ ANALYSIS OF THREE-BODY B DECAYS

A. GARMASH

(for the Belle Collaboration)

*Department of Physics, Princeton University,
Princeton, NJ 08544, U.S.A.*



Results on Dalitz analysis of three-body charmless $B^+ \rightarrow K^+\pi^+\pi^-$ and $B^+ \rightarrow K^+K^+K^-$ decays are reported. We also present preliminary results on the studies of direct CP violation in three-body decay $B^\pm \rightarrow K^\pm\pi^+\pi^-$. The analysis is performed using a large data sample collected with the Belle detector.

1 Introduction

Studies of B meson decays to three-body charmless hadronic final states are a natural extension of studies of decays to two-body charmless final states. Multiple resonances occurring nearby in phase space will interfere and a full amplitude analysis is required to extract correct branching fractions for the intermediate quasi-two-body states. In addition to being a rich laboratory for studying B meson decay dynamics, three-body charmless hadronic final states may provide new possibilities for CP violation searches¹.

2 Apparatus, Data Sample & Event Selection

This analysis is based on a 140 fb^{-1} data sample (152 million $B\bar{B}$ pairs) used for Dalitz analysis and on a 253 fb^{-1} data sample (274 million $B\bar{B}$ pairs) used for searches for direct CP violation in decay $B^\pm \rightarrow K^\pm\pi^+\pi^-$. The data are collected with the Belle detector operating at the KEKB asymmetric-energy e^+e^- collider with a center-of-mass energy at the $\Upsilon(4S)$ resonance.

The Belle detector² is a large-solid-angle magnetic spectrometer based on a 1.5 T superconducting solenoid magnet. Charged particle tracking is provided by a three-layer silicon vertex detector and a 50-layer central drift chamber (CDC) that surround the interaction point. Charged hadron identification is provided by dE/dx measurements in the CDC, an array of

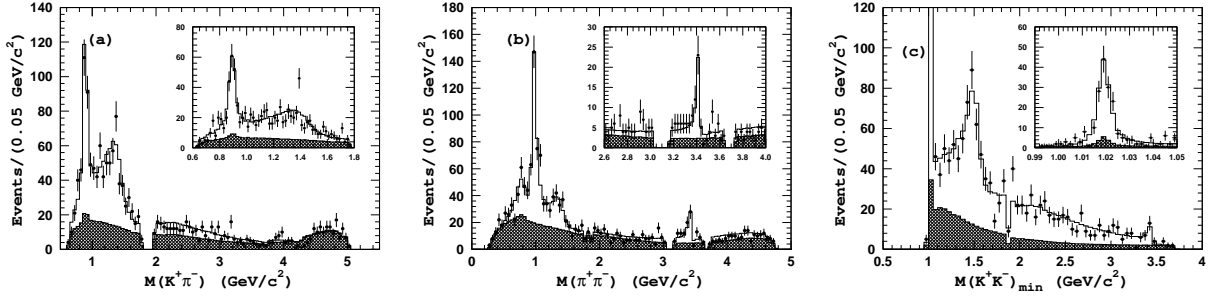


Figure 1: Two-particle invariant mass spectra for events in the B signal region (open histograms) and for background events in the $\Delta E - M_{bc}$ sidebands (hatched histograms). (a) $M(K^+\pi^-)$ spectrum with $M(\pi^+\pi^-) > 1.5 \text{ GeV}/c^2$; (b) $M(\pi^+\pi^-)$ with $M(K^+\pi^-) > 2.0 \text{ GeV}/c^2$ and (c) $M(K^+K^-)_{\min}$.

1188 aerogel Čerenkov counters (ACC), and a barrel-like array of 128 time-of-flight scintillation counters (TOF); information from the three subdetectors is combined to form a single likelihood ratio, which is then used for pion, kaon and proton discrimination. For charged kaon identification, we impose a requirement on the particle identification variable that has 86% efficiency and a 7% fake rate from misidentified pions. Charged tracks that are positively identified as electrons or protons are excluded from the analysis.

The dominant background to studied processes is due to $e^+e^- \rightarrow q\bar{q}$ ($q = u, d, s$ and c quarks) continuum events. This type of background is suppressed using variables that characterize the event topology. This allows to reject about 98% (92%) of the continuum background in the $B^\pm \rightarrow K^\pm\pi^+\pi^-$ ($B^\pm \rightarrow K^\pm K^+K^-$) decay while retaining 36% (70%) of the signal. A detailed description of the continuum suppression technique can be found in Ref. ³ and references therein. The background that originates from other B meson decays is studied using a large sample of Monte Carlo generated events. We find that the dominant $B\bar{B}$ background in the $K^+\pi^+\pi^-$ final state is due to $B^+ \rightarrow \bar{D}^0\pi^+$, $\bar{D}^0 \rightarrow K^+\pi^-$ and also $B^+ \rightarrow J/\psi(\psi(2S))K^+$, $J/\psi(\psi(2S)) \rightarrow \mu^+\mu^-$ decays. We veto these events by requiring $|M(K\pi) - M_D| > 0.10 \text{ GeV}/c^2$, $|M(\pi^+\pi^-)_{\mu^+\mu^-} - M_{J/\psi}| > 0.07 \text{ GeV}/c^2$ and $|M(\pi^+\pi^-)_{\mu^+\mu^-} - M_{\psi(2S)}| > 0.05 \text{ GeV}/c^2$, where subscript $\mu^+\mu^-$ indicates that the muon mass assignment was used for charged tracks to calculate the two-particle invariant mass. We also remove $B^+ \rightarrow \bar{D}^0 K^+$, $\bar{D}^0 \rightarrow \pi^+\pi^-$ signal by requiring $|M(\pi^+\pi^-) - M_D| > 15 \text{ MeV}/c^2$. To suppress the background due to π/K misidentification, we also exclude candidates if the invariant mass of any pair of oppositely charged tracks from the B candidate is consistent with the $\bar{D}^0 \rightarrow K^+\pi^-$ hypothesis within $15 \text{ MeV}/c^2$, regardless of the particle identification information. The most significant background from charmless B decays is found to originate from $B^+ \rightarrow \eta' K^+$ followed by $\eta' \rightarrow \pi^+\pi^-\gamma$, $B^+ \rightarrow \rho^0\pi^+$ and $B^0 \rightarrow K^+\pi^-$ decays. These backgrounds cannot be removed and are taken into account when fitting the data.

The dominant background to the $K^+K^+K^-$ final state from other B decays is due to $B \rightarrow Dh$ process, where h stands for a charged pion or kaon. To suppress this background, we reject events where any two-particle invariant mass is consistent with $\bar{D}^0 \rightarrow K^+K^-$ or $\bar{D}^0 \rightarrow K^+\pi^-$ within $15 \text{ MeV}/c^2$ regardless of the particle identification information. We find no charmless B decay modes that produce a significant background to the $K^+K^+K^-$ final state.

3 Results on Dalitz Analysis of $B^+ \rightarrow K^+\pi^+\pi^-$ and $B^+ \rightarrow K^+K^+K^-$

Results of this analysis are described in detail in Ref. ³. There are 2584 $K^\pm\pi^+\pi^-$ and 1400 $K^\pm K^+K^-$ events in the B signal region that satisfy all the selection requirements. Two-body invariant mass distributions for these events are shown in Fig. 1. We find that the best fit to $K^\pm\pi^+\pi^-$ events is obtained with a matrix element that is a coherent sum of the $K^*(892)^0\pi^+$, $K_0^*(1430)^0\pi^+$, $\rho(770)^0 K^+$, $f_0(980)K^+$, $f_X(1300)K^+$, $\chi_{c0}K^+$ quasi-two-body channels and a

Table 1: Summary of branching fraction results. The first quoted error is statistical, the second is systematic and the third is the model error.

Mode	$\mathcal{B}(B^+ \rightarrow Rh^+) \times \mathcal{B}(R \rightarrow h^+h^-) \times 10^6$	$\mathcal{B}(B^+ \rightarrow Rh^+) \times 10^6$
$K^\pm \pi^+ \pi^-$ charmless total	–	$46.6 \pm 2.1 \pm 4.3$
$K^*(892)^0 \pi^+, K^*(892)^0 \rightarrow K^+ \pi^-$	$6.55 \pm 0.60 \pm 0.60^{+0.38}_{-0.57}$	$9.83 \pm 0.90 \pm 0.90^{+0.57}_{-0.86}$
$K_0^*(1430)^0 \pi^+, K_0^*(1430)^0 \rightarrow K^+ \pi^-$	$27.9 \pm 1.8 \pm 2.6^{+8.5}_{-5.4}$	$45.0 \pm 2.9 \pm 6.2^{+13.7}_{-8.7}$
$K^*(1410)^0 \pi^+, K^*(1410)^0 \rightarrow K^+ \pi^-$	< 2.0	–
$K^*(1680)^0 \pi^+, K^*(1680)^0 \rightarrow K^+ \pi^-$	< 3.1	–
$K_2^*(1430)^0 \pi^+, K_2^*(1430)^0 \rightarrow K^+ \pi^-$	< 2.3	–
$\rho(770)^0 K^+, \rho(770)^0 \rightarrow \pi^+ \pi^-$	$4.78 \pm 0.75 \pm 0.44^{+0.91}_{-0.87}$	$4.78 \pm 0.75 \pm 0.44^{+0.91}_{-0.87}$
$f_0(980)K^+, f_0(980) \rightarrow \pi^+ \pi^-$	$7.55 \pm 1.24 \pm 0.69^{+1.48}_{-0.96}$	–
$f_2(1270)K^+, f_2(1270) \rightarrow \pi^+ \pi^-$	< 1.3	–
Non-resonant	–	$17.3 \pm 1.7 \pm 1.6^{+17.1}_{-7.8}$
$K^\pm K^+ K^-$ charmless total	–	$30.6 \pm 1.2 \pm 2.3$
$\phi K^+, \phi \rightarrow K^+ K^-$	$4.72 \pm 0.45 \pm 0.35^{+0.39}_{-0.22}$	$9.60 \pm 0.92 \pm 0.71^{+0.78}_{-0.46}$
$\phi(1680)K^+, \phi(1680) \rightarrow K^+ K^-$	< 0.8	–
$f_0(980)K^+, f_0(980) \rightarrow K^+ K^-$	< 2.9	–
$f_2'(1525)K^+, f_2'(1525) \rightarrow K^+ K^-$	< 4.9	–
$a_2(1320)K^+, a_2(1320) \rightarrow K^+ K^-$	< 1.1	–
Non-resonant	–	$24.0 \pm 1.5 \pm 1.8^{+1.9}_{-5.7}$
$\chi_{c0}K^+, \chi_{c0} \rightarrow \pi^+ \pi^-$	$1.37 \pm 0.28 \pm 0.12^{+0.34}_{-0.35}$	–
$\chi_{c0}K^+, \chi_{c0} \rightarrow K^+ K^-$	$0.86 \pm 0.26 \pm 0.06^{+0.20}_{-0.05}$	–
$\chi_{c0}K^+$ combined	–	$196 \pm 35 \pm 33^{+197}_{-26}$

non-resonant component. A channel $f_X(1300)K^+$ (with mass and width of $f_X(1300)$ to be determined from the fit) is added to account for an excess of signal events visible in $M(\pi^+\pi^-)$ spectrum near 1.3 GeV/ c^2 . Results of the best fit are shown in Figs. 1 (a,b). The mass and width of the $f_X(1300)$ state obtained from the fit are consistent with those for the $f_0(1370)$, however more data are required for more definite conclusion. To test for the contribution of other possible quasi-two-body intermediate states such as $K^*(1410)^0 \pi^+$, $K^*(1680)^0 \pi^+$, $K_2^*(1430)^0 \pi^+$ or $f_2(1270)K^+$, we include an additional amplitude of each of these channels in the matrix element one by one and repeat the fit to data. None of these channels have a statistically significant signal. Branching fraction and upper limit results are summarized in Table 1.

The best fit to $K^\pm K^+ K^-$ events is obtained with a matrix element that is a coherent sum of the ϕK^+ , $f_X(1500)K^+$, $\chi_{c0}K^+$ quasi-two-body channels and a non-resonant component, where the $f_X(1500)K^+$ (with mass and width of $f_X(1300)$ to be determined from the fit) channel is added to describe the excess of signal events visible in $K^+ K^-$ mass spectrum near 1.5 GeV/ c^2 . As there are two identical kaons in the final state, the decay amplitude is symmetrized with respect to interchange of two kaons of the same charge. Results of the fit are shown in Fig. 1 (c) and summarized in Table 1. In order to check the sensitivity of the data to the spin of the $f_X(1500)$ state, we replace the scalar amplitude by a vector or a tensor amplitude for the $f_X(1500)$: the scalar hypothesis gives the best fit. To estimate the possible contribution from other quasi-two-body channels, we include an additional decay channel and repeat the fit to the data. In particular we test the $\phi(1680)K^+$, $f_2'(1525)K^+$ and $a_2(1320)K^+$ channels. In all cases the fit finds no statistically significant signal for the newly added channel. Since we observe a clear $f_0(980)K^+$ signal in the $K^+ \pi^+ \pi^-$ final state, we try to include the $f_0(980)K^+$ amplitude in the $B^+ \rightarrow K^+ K^+ K^-$ matrix element as well: no statistically significant contribution from this channel is found.

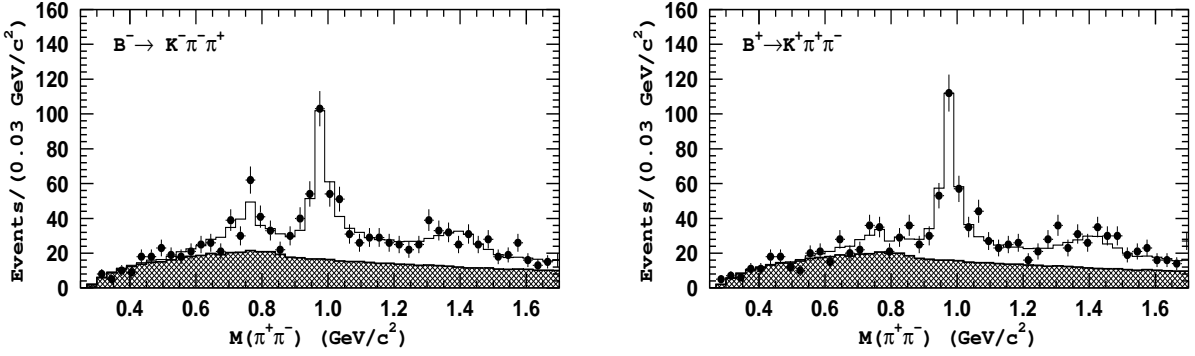


Figure 2: $M(\pi^+\pi^-)$ mass spectra for B^- (left) and B^+ (right). Points with error bars are data, the open histogram is the fit result and the hatched histogram is the background component.

4 Search for Direct CP Violation in $B^\pm \rightarrow K^\pm \pi^+ \pi^-$

In the analysis of the direct CP violation in $B^\pm \rightarrow K^\pm \pi^+ \pi^-$ decays we use larger data sample of 253 fb^{-1} . To search for direct CP violation we make a fit to $K^-\pi^-\pi^+$ and $K^+\pi^+\pi^-$ samples separately. In the fit to B^- and B^+ subsamples we fix all the parameters not sensitive to CP violation (such as masses and widths of resonance states) at values determined from the fit to the combined B^\pm sample. Results of calculations of CP violation asymmetries defined as

$$A_{\text{CP}} = \frac{\mathcal{B}(B^- \rightarrow f^-) - \mathcal{B}(B^+ \rightarrow f^+)}{\mathcal{B}(B^- \rightarrow f^-) + \mathcal{B}(B^+ \rightarrow f^+)} \quad (1)$$

are given in Table 2. In all except for $B^\pm \rightarrow \rho(770)^0 K^\pm$ channels the measured asymmetry agrees with zero within $1\sigma - 1.5\sigma$ (after the model uncertainty is accounted). A 2.4σ hint for a large direct CP violation is observed in the decay $B^\pm \rightarrow \rho(770)^0 K^\pm$. This is demonstrated in Fig. 2, where the $\pi^+\pi^-$ invariant mass distribution for the $\rho(770) - f_0(980)$ mass region is shown. Analysis with a large data sample is required in order to check this result.

Table 2: Results of A_{CP} calculation. Quoted errors are statistical, systematic and the model related error.

Mode	A_{CP}
$K^\pm \pi^+ \pi^-$ Charmless	$0.046 \pm 0.030 \pm 0.02$
$K^*(892)^0 \pi^+, K^*(892)^0 \rightarrow K^+ \pi^-$	$-0.14 \pm 0.08 \pm 0.02^{+0.03}_{-0.07}$
$K_0^*(1430) \pi^+, K_0^*(1430)^0 \rightarrow K^+ \pi^-$	$+0.06 \pm 0.05 \pm 0.02^{+0.01}_{-0.32}$
$\rho(770)^0 K^+, \rho(770)^0 \rightarrow \pi^+ \pi^-$	$+0.27 \pm 0.12 \pm 0.02^{+0.59}_{-0.03}$
$f_0(980) K^+, f_0(980) \rightarrow \pi^+ \pi^-$	$-0.13 \pm 0.11 \pm 0.02^{+0.16}_{-0.06}$
Non-resonant	$-0.04 \pm 0.08 \pm 0.02^{+0.16}_{-0.03}$
$\chi_{c0} K^+, \chi_{c0} \rightarrow \pi^+ \pi^-$	$-0.30 \pm 0.22 \pm 0.02^{+0.42}_{-0.00}$

References

1. See for example: G. Eilam, M. Gronau and R.R. Mendel, *Phys. Rev. Lett.* **74**, 4984 (1995); S. Fajfer, R.J. Oakes, and T.N. Pham, *Phys. Lett. B* **539**, 67 (2002); N.G. Deshpande, N. Sinha and R. Sinha, *Phys. Rev. Lett.* **90**, 061802 (2003); M. Gronau, *Phys. Rev. Lett.* **91**, 139101 (2003); T. Gershon and M. Hazumi, *Phys. Lett. B* **596**, 163 (2004).
2. A. Abashian *et al.*, *Nucl. Instrum. Methods A* **479**, 117 (2002).
3. A. Garmash *et al.* (Belle Collaboration), hep-ex/0412066.